19 Technology Program Accomplishments

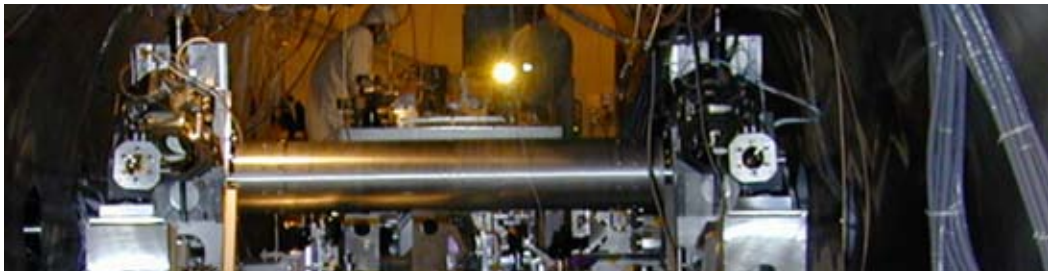

Bijan Nemati (JPL), **Inseob Hahn** (JPL), and **Oscar S. Alvarez-Salazar** (JPL)

ABSTRACT

Developed over the past 12 years, SIM Lite's spectacularly successful technology program has conclusively demonstrated that the era of sub-μas optical astrometry is at hand. Overall, SIM Lite's development has placed a high emphasis on retiring risks and ensuring completeness. This resulted in the successful completion of all of the NASA-required technical milestones. With many key brassboards already completed and submitted to environmental testing, and more presently under development, SIM Lite is ready for final design and flight implementation.

19.1 Technology Demonstrated Through Testbeds

For over a decade, the SIM Project has carried out an expansive and ambitious technology program to demonstrate the key technologies required in order to make sub-μas astrometry possible. The program has been a resounding success. Here we give a brief overview of the measurement approach, the technologies required, and the results obtained from SIM Lite's technology program.

The flowdown of the error budget showed, early on, that in many areas the technology for SIM Lite had yet to be demonstrated. Some of the most demanding technology included:

- Measurement of displacements within the instrument to picometers — 2 orders of magnitude better than the current state of the art.
- Pathlength stabilization to nanometers in the presence of various disturbances in the spacecraft environment.
- Nanometer pathlength stabilization when the star is so dim that the fringe position can only be estimated every few minutes.
- Millikelvin-level thermal stability for the collector optics.
- Building a star tracker with 50 μas accuracy — 3 orders of magnitude better than the state of the art.

This chapter highlights how these and other technology challenges were successfully met and retired by SIM LIte's technology program.

Broadly speaking, the SIM technology testbeds can be placed in two categories. The first is focused on whether the level of pm-level sensing required for SIM Lite astrometry can be achieved. Chief among these are the Microarcsecond Metrology (MAM), the external metrology (Kite), and the Guide-2 telescope (G2T) testbeds. The second category is focused on the environment under which these measurements need to take place. The primary concerns here are vibrations and thermal variations. To address the dynamics and controls issues, a series of system-level testbeds was created, culminating in the three-baseline System-Level Testbed (STB-3). Thermo-opto-mechanical (TOM) investigations were conducted with the TOM testbed. We will discuss STB-3 and TOM later in this chapter.

19.2 The Microarcsecond Metrology Testbed

The MAM testbed, shown in Figure 19-1**,** was designed to study specific errors expected in SIM Lite's pm-class interferometers. It demonstrates, at the system level, the essential technology for sensing the white light and metrology pathlength differences at the pm level. The MAM testbed tested most of the error budget allocations for the science and the guide interferometers at the system level.

The testbed, whose layout appears in Figure 19-2, is composed of two major parts: the test article and the pseudo star. The test article (TA) is an optical interferometer with internal metrology. The inverse interferometer pseudo star (IIPS) provides the test article with wavefronts consistent with a distant star. Starting from the IIPS source, broadband (600 to 1000 nm) light is injected from an optical fiber tip, then collimated and separated into two beams. The beams are steered to two coordinated stages and thence launched towards the test article siderostats as flat, coherent wavefronts. The stages are designed to provide simulated starlight for the test article over the range of angles that comprises SIM Lite's field of regard (FOR), a 15-degree-diameter circle on the sky. The wavefronts are not required to have the relative delay that corresponds to the angle of the star being simulated. The actual external delay generated by IIPS is monitored by its metrology system, and it is the job of the test article to measure this delay.

Figure 19-1. SIM Lite's MAM testbed, shown here in the 4-m-diameter vacuum chamber, has demonstrated goal-level performance (see text) in both narrow-angle and wide-angle regimes. (From Hines et al. 2003.)

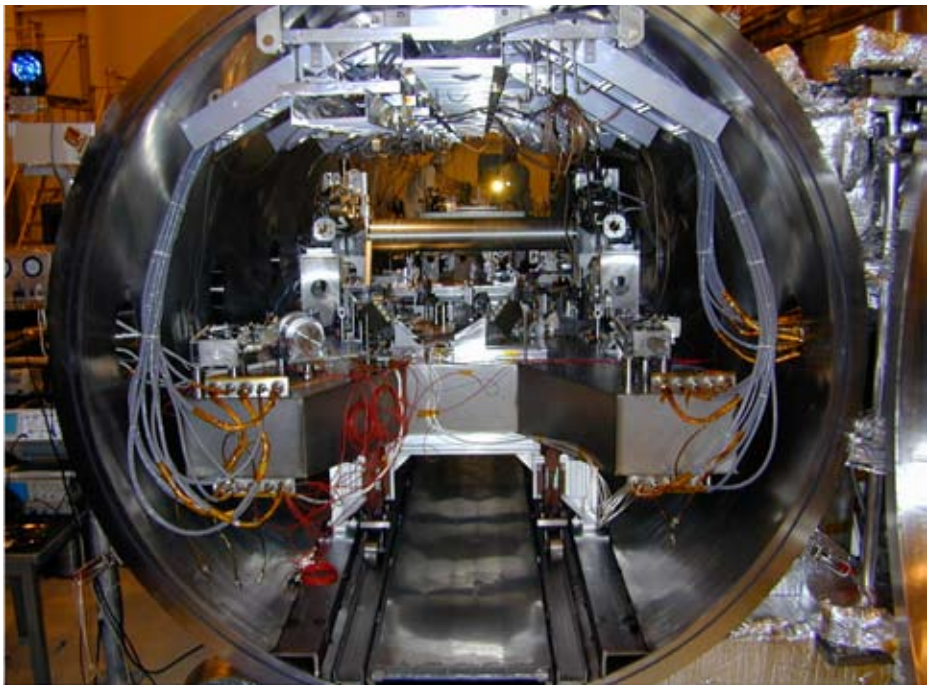

Figure 19-2. The MAM optical system captures the main elements of the SIM Lite science interferometer. (From Hines et al. 2003.)

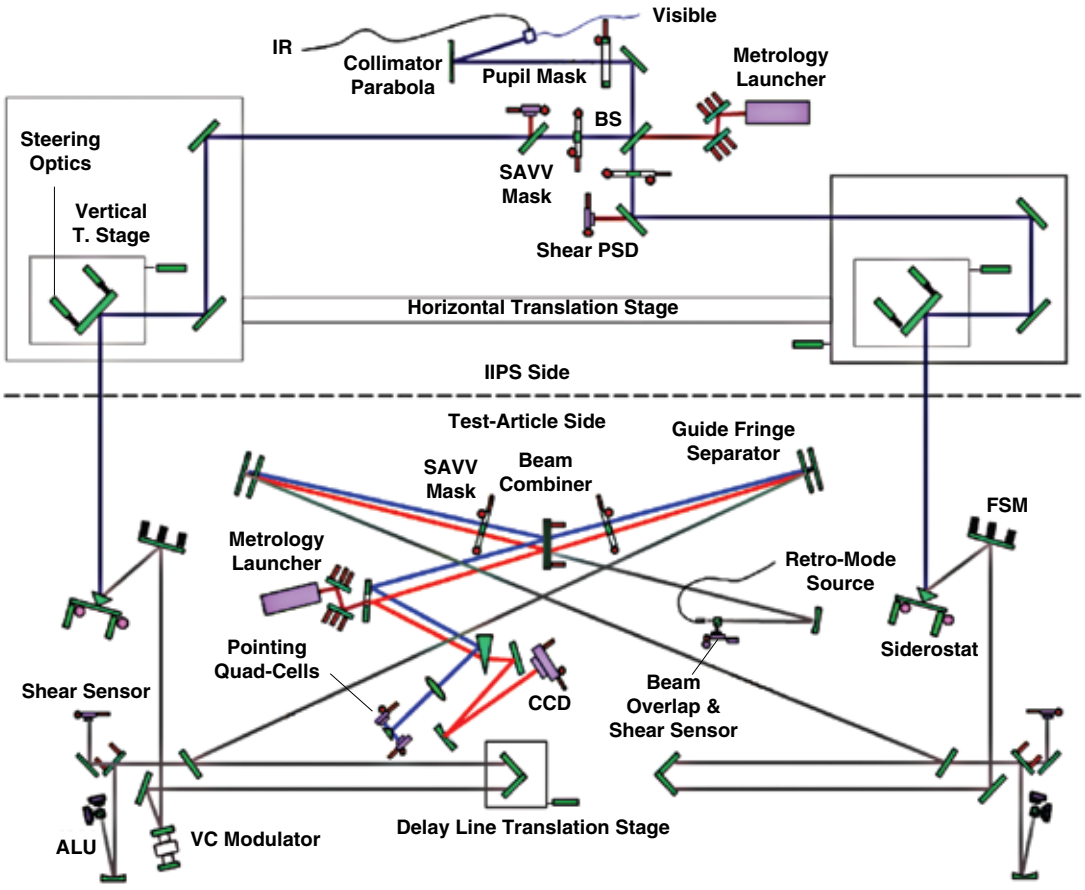

In the interferometer, the two "starlight" beams captured by the siderostats are steered to a beam splitter where they are combined and spectrally dispersed onto a CCD detector. The pathlength of one interferometer arm is modulated using a triangle wave resulting in an intensity modulation detected on the fringe tracking CCD. By proper detection and processing of this intensity signal, the phase of the white light fringe pattern can be measured at the pm level. Thus, the white light beams start at the IIPS beam splitter and terminate at the TA beam combiner. As in SIM Lite, the fundamental reference points of the TA interferometer are the vertices of the two corner cubes installed at the center of the two siderostats: all astrometric measurements are defined in terms of these two points.

Besides the white light, the same paths are also traveled by metrology, though not continuously. MAM uses prototype internal metrology launchers called SAVV (short for sub-aperture vertex-to-vertex). The experience gained from the SAVV launchers led to the development of the successful internal metrology brassboard beam launcher (Chapter 20). In MAM, a metrology launcher in the IIPS monitors the left-right path difference from the IIPS beam splitter up to the TA siderostat-mounted corner cubes (Figure 19-3). The TA internal metrology does the same thing starting from the TA beam combiner out to the siderostat corner cubes. A severe technical constraint on MAM, as on SIM Lite, is that the metrology and starlight paths have different footprints. The starlight beam footprint is an annulus around a central metrology footprint. Achieving pm-level internal metrology fidelity with respect to starlight in the presence of this constraint necessitates careful optical design and accurate alignment.

The MAM error metric is the difference between the total white light and metrology measurements:

$$E_{MAM} = \phi_{TA} - (M_{IIPS} + M_{TA}) \quad (1)$$

The TA fringe measurement gives the total pathlength difference from the IIPS beam splitter to the TA beam combiner [the conversion from phase to pathlength units is implied in Equation (1)]. The sum of the IIPS and TA metrology also gives a measurement of the total path difference. As usual, these are all variation ("relative") measurements over some given time span. Going from the error metric to the narrow-angle and grid performance metrics occurs by following the appropriate scenarios and their associated processing algorithms. Since the performance metrics are based on the instrument only, an adjustment of $1/\sqrt{2}$ is applied to the error metric. This factor assumes that the IIPS and TA interferometers have similar errors so that the variance of the error metric (Equation 1) is twice the variance of the TA portion.

In MAM's wide-angle (WA) runs, the pseudo star projects planar wavefronts at various angles consistent with SIM Lite's 15 degree FOR. The starting point is a star at the middle of the field. Over the course of a one-hour sequence of measurements representing a tile, the initial star is measured again at the middle of the hour and once more at the end. These three visits are used to remove the linear portion of any temporal drift in the data. In the MAM runs, certain stars in the field are designated as grid stars. These are used to calibrate out those trends in the field that the grid solution is expected to solve for. The MAM wide-angle metric is the root-mean-square (RMS) residual for stars not used to determine the field-dependent trend. The wide-angle error in MAM was measured to be under 260 pm, which is better than the goal performance for SIM Lite.

The geometry of a typical SIM Lite narrow-angle (NA) visit is shown in Figure 19-4. To minimize systematic errors, the reference stars are chosen so that their collective center of brightness (computed analogously to a center of mass) is as close as possible to the target star. On the other hand, to minimize random errors, the reference stars are allowed to be as far as one degree from the target star to increase the likely presence of brighter reference stars. During each visit, the baseline points in a single direction. In order to measure the target motion in two angles, successive visits use alternate (ideally orthogonal) baseline orientations.

Figure 19-3. The SAVV beam launcher, used for the first time in MAM, proved that pm-class internal metrology is feasible. It became the prototype for SIM Lite's brassboard beam launcher.

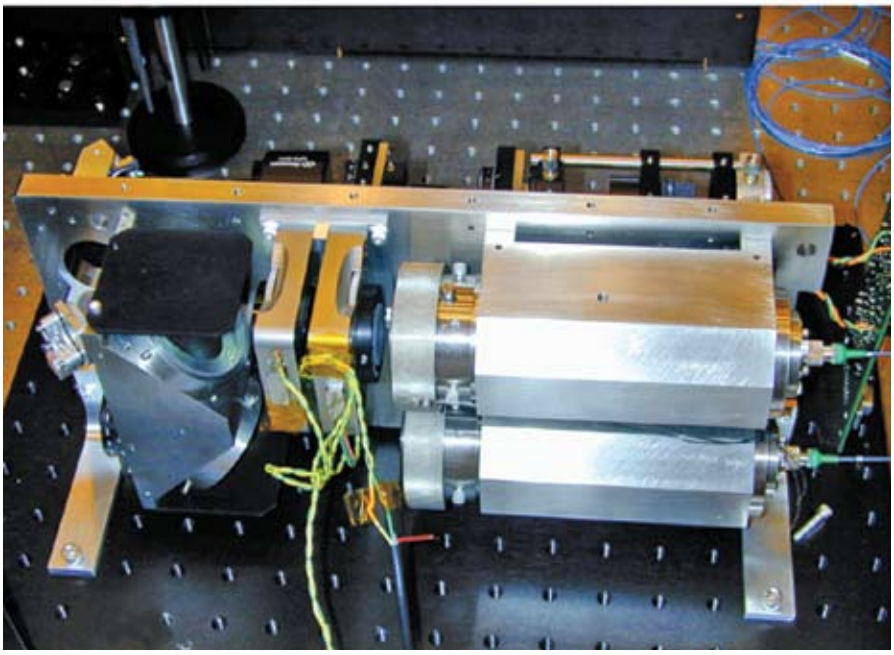

Figure 19-4. The narrow-angle observing scenario with a target star at the center of the field of regard and reference stars within a circle of one-degree radius. The baseline orientation on a subsequent visit would be orthogonal to that shown here.

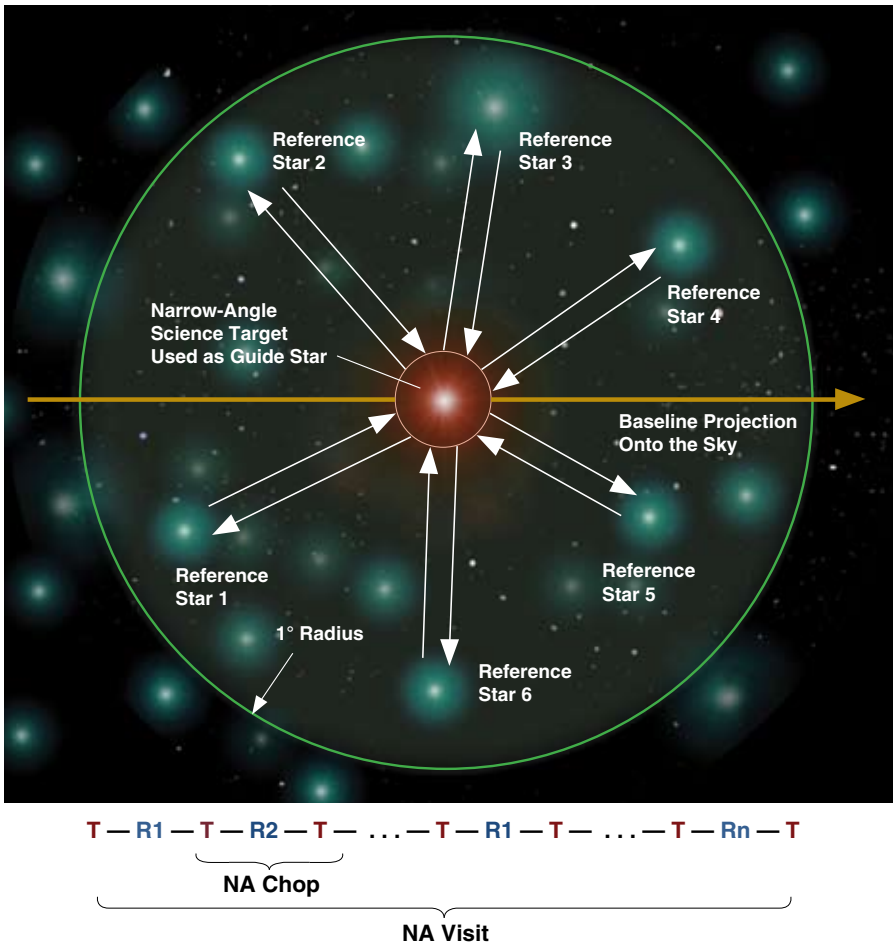

The basic NA measurement is the delay difference between the target and a reference star. In order to minimize the effect of instrument drifts, the instrument chops between the target and a reference and back to the target. The chopped delay difference is then given by:

$$d_i = x_R^j - \frac{x_T^{i-1} + x_T^{i+1}}{2} \tag{2}$$

where x_R^j is the measured delay for reference star *i*. It includes corrections for proper motion and parallax effective at the measurement epoch. Similarly, x_T^{i-1} and x_T^{i+1} are the measured residual delays in the preceding and succeeding target looks, respectively. Depending on the brightness of the star, each observation is approximately 30 seconds long and the time to look from a target star to a reference star is approximately 15 seconds. The entire cycle of observations is repeated during the visit, so that each reference star is measured twice. These are then averaged, forming a single, per-visit delay difference between the target and each reference star. The differences are collectively analyzed to determine the motion of the brightness center of the reference stars relative to the local origin, which is defined to be the location of the target star. Thus, the signal is the relative motion of the reference star brightness center from epoch to epoch. For planet detection, the signal is in fact the acceleration measured across many epochs.

MAM NA visits involve four stars in a symmetric cross pattern. The goal-level NA performance for MAM, based on the SIM Lite error budget, is that the per-visit error be under 24 pm in at least 68.3 percent of the runs. In actual tests, the fraction of runs with performance metric under 24 pm was found to be 67.8 percent, implying performance just meeting the goal.

In a follow-on version of the MAM testbed, called Spectral Calibration Development Unit (SCDU), the field-independent portion of the NA performance was recently studied in a 230-hour quasi-static run. The data were divided up into segments ascribed alternately to target and reference star looks, as well as slew times between the looks where the data were not used. Chop differences in the manner of Equation (2) were computed. Figure 19-5 shows the effectiveness of averaging the chops. As can be seen in the figure, averaging continues to reduce the error until all available data are exhausted. Hence, no noise floor is reached using the total recorded data, dipping the error to below 17 nanoarcseconds after 71 hours of integration.

An important question in applying testbed results to SIM Lite is: How does the thermal behavior of the relevant parts of SIM Lite compare with the testbed? Figure 19-6 shows a comparison of the temperature power spectral densities (PSDs) as measured in the testbed and modeled for SIM Lite. The SIM Lite model is a 20-hour simulation with a few thousand nodes. The temperatures extracted are those associated with the beam combiner region, where the internal metrology beam originates. The relevant frequency range for planet finding and NA astrometry is near 1/90 s or about 0.01 Hz. Overall, the plot shows the expected thermal environment for SIM Lite to be no worse than that experienced by the testbed. Thus, the testbed shows end-of-mission error at or below 17 nanoarcseconds with thermal conditions more challenging than SIM Lite is expected to encounter.

19.3 The External Metrology Truss Testbed (Kite)

SIM Lite's external metrology truss testbed was built to demonstrate that an external metrology system with pm-level performance is feasible for SIM Lite. A metrology truss consists of a set of fiducials, typically hollow corner cubes, with metrology beam launchers interposed between them. Each beam launcher, along with its associated laser source and phase measurement electronics, comprises a

Figure 19-5. The narrow-angle chopping scheme is highly effective in randomizing the thermal error. The error behaves as white noise down, down to 17 nanoarcseconds after 71 hours of integration.

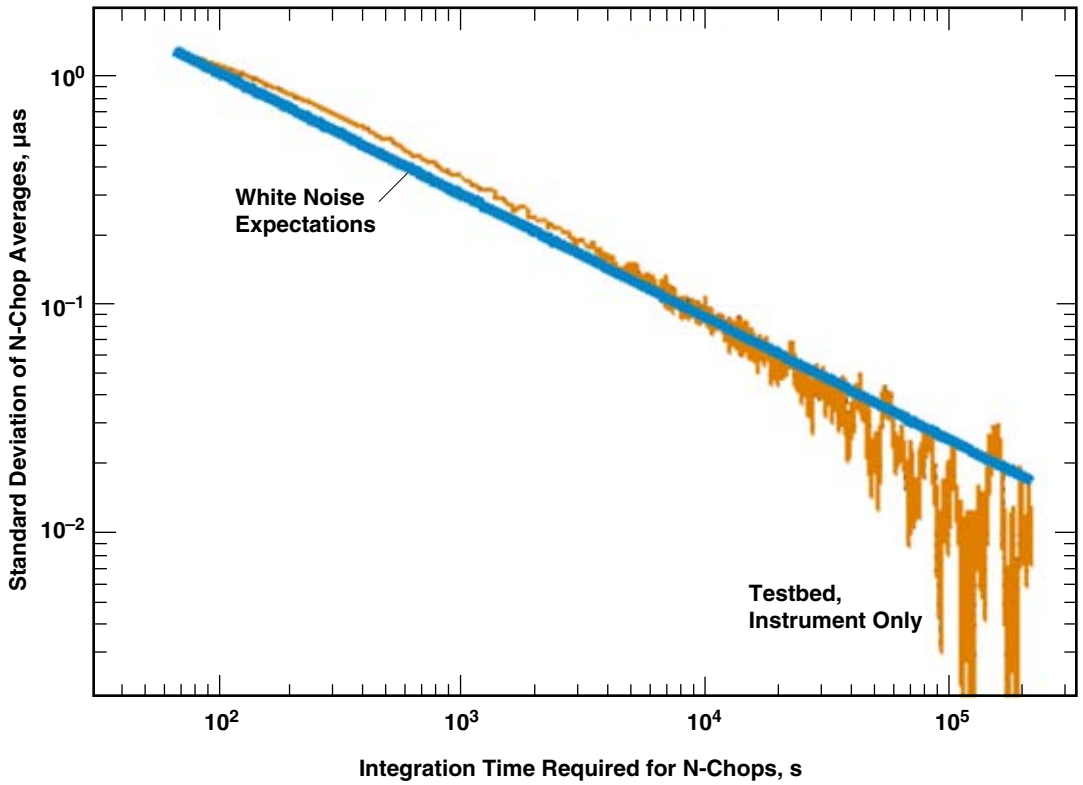

Figure 19-6. The SIM Lite expected thermal environment (blue) is quieter and more benign than the thermal environment encountered by the testbed (orange).

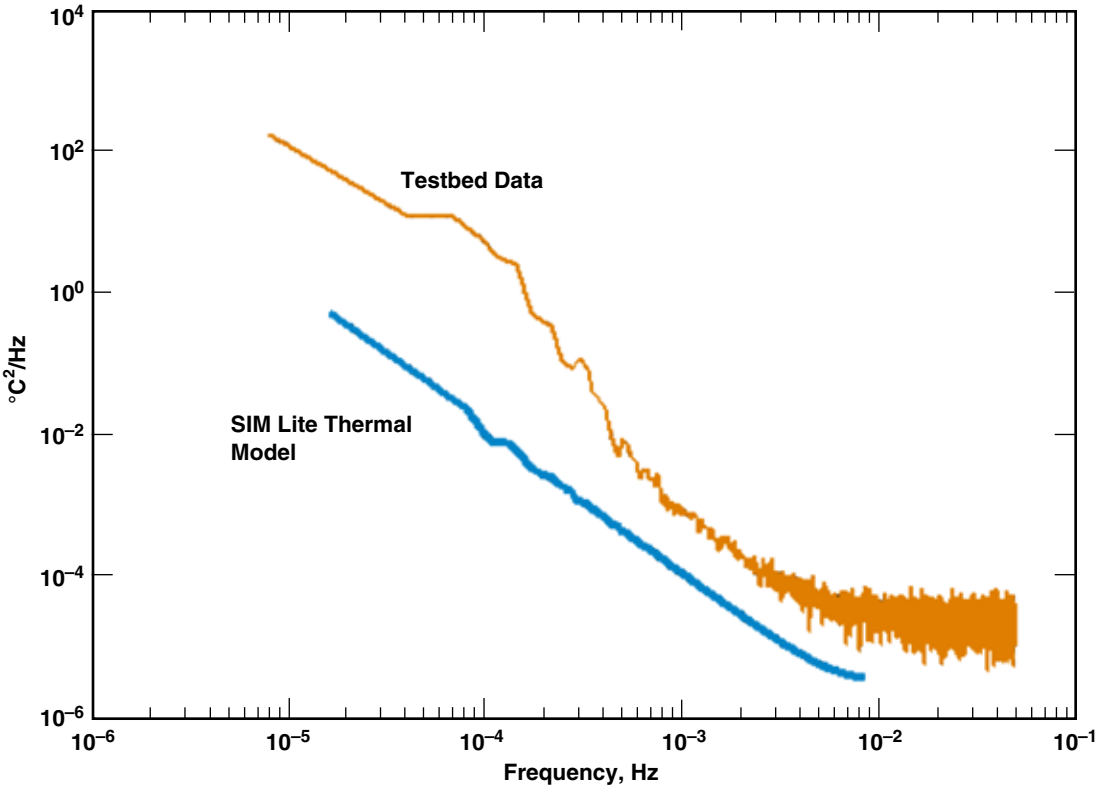

one-dimensional metrology gauge. The testbed featured a novel beam launcher, called QP for "quick prototype," in which the reference and probe beams were spatially separated (Figure 19-7). This innovation made possible the first feasible pm-class metrology gauges.

The minimal test configuration for point-to-point metrology is a two-gauge set-up, in which two metrology beam launchers simultaneously probe the same pair of corner cubes, as shown in Figure 19-8. Assuming the gauges are independent, the difference between their readings will have a variance that is twice the per-gauge variance. The two gauge set-up can be used to qualify individual launchers for most of the field-independent errors discussed in Chapter 18.

A real truss, however, will have errors beyond the reach of a two-gauge test. The entire class of field-dependent errors, as well as truss-only errors such as in the absolute metrology survey, needed to be investigated. For a truss with N nodes (fiducials), the number of possible links and the number of sensed degrees of freedom are given by:

$$n_{link} = \frac{N(N-1)}{2} \quad \text{vs.} \quad n_{dof} = \begin{cases} 2N-3 & \text{(2 dimensions)} \\ 3N-6 & \text{(3 dimensions)} \end{cases} \tag{3}$$

To have redundancy, i.e., $n_{link} > n_{dof}$, the minimal configuration is a two-dimensional truss with four nodes, where there are six links, or measurements, and five sensed degrees of freedom, or unknowns. Hence, the testbed was chosen as a planar truss with four nodes. Its original diamond shape led to the name "Kite." Figure 19-9 shows the testbed in its original configuration in the vacuum tank it shared with the MAM testbed. To achieve planarity, a theodolite was used to move one of the four corner cubes (called the planarity corner cube) into the plane defined by the other three. A planarity error of less than a few tens of microns is sufficient to keep the resulting truss error at the allocated level of a few pm.

To illustrate the testbed data and the impact of narrow-angle processing, a sample one-hour quasi-static run is shown in Figure 19-10. Quasi-static conditions imply that no intentional change or disturbance was introduced to the test set-up. The dominant sources of motion under these conditions are vibrations and ambient thermal variations. The sampling rate in the test shown here is 100 Hz, with 10 ms averaging of the metrology data prior to readout. The green trace, extending lower than all others, is telemetry from Gauge 2, or the test link. It shows a hash of about 30 nm RMS from vibrations on top of a slower trend of approximately 400 nm peak to peak from temperature change during this period.

The error metric for the truss testbed is the difference between the readings of Gauge 2 versus the prediction for that link using the other five gauges. This prediction will rely on a prior survey of the absolute lengths at the <10 μm level. The truss is operated in "absolute" mode periodically to obtain an up-to-date survey suitable for pm-level relative metrology. For this geometry, modeling shows that the per-link expected error is very nearly $1/\sqrt{2}$ of the metric error. The metric error is the black trace.

It is possible to use quasi-static data such as these to assess aspects of truss performance under various scenarios. For example, one can apply processing representative of the narrow-angle scenario. Figure 19-11 shows the error averaged down in 30-second intervals, resulting in the blue trace. The peak to peak variation in the averaged metric is seen to be about 400 pm over the hour. However, the timescale for a narrow-angle chop measurement is much shorter. The green trace shows the single-chop error over the same time span, with a standard deviation of 15 pm. Assuming four reference stars each visited twice, the effective random error is reduced by averaging, as shown by the red dots whose standard deviation is 8 pm.

In Kite's full narrow-angle tests, four reference stars are assumed to be symmetrically situated 1 degree away from the target star in a cross pattern. For the corner cube, this means rotations to 0.5 degree

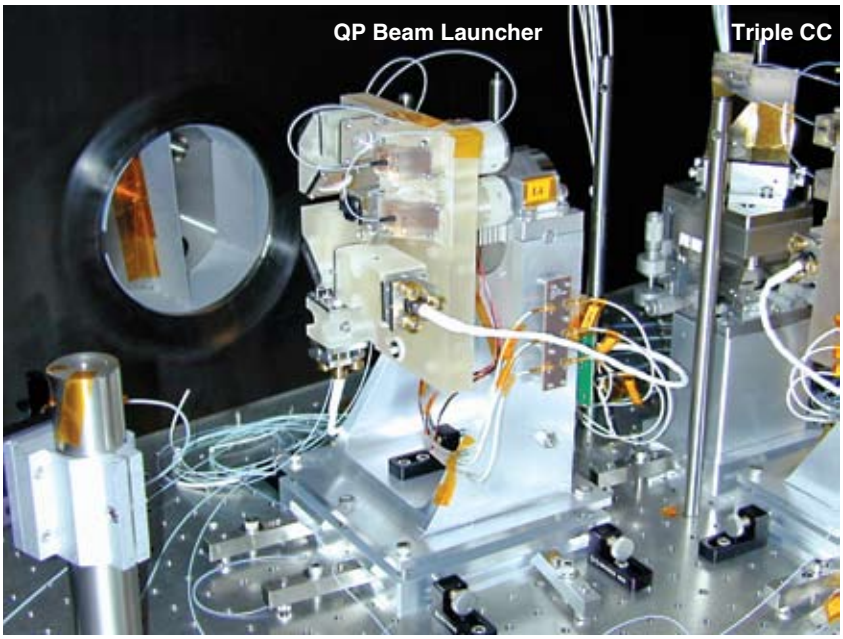

Figure 19-7. The quick prototype (QP) beam launcher demonstrated for the first time that pm-level monitoring of relative displacements between two fiducials is feasible. It also demonstrated absolute metrology at the 10 micron level. In the figure, CC refers to corner cube.

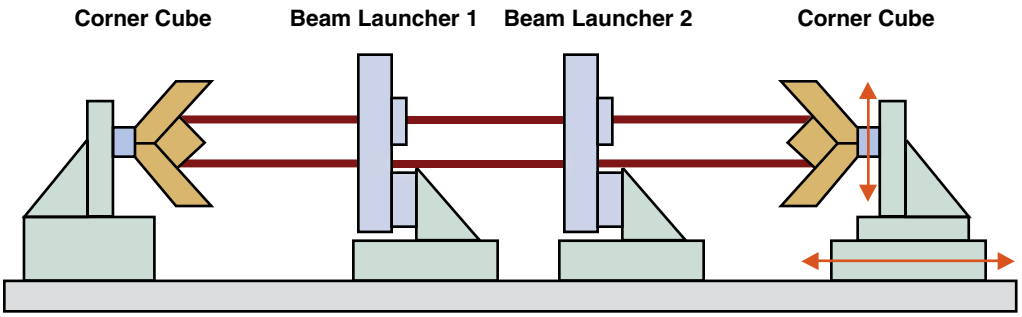

Figure 19-8. To accommodate a two-gauge test set-up, SIM Lite beam launchers are designed so that both have clear paths to the corner cubes.

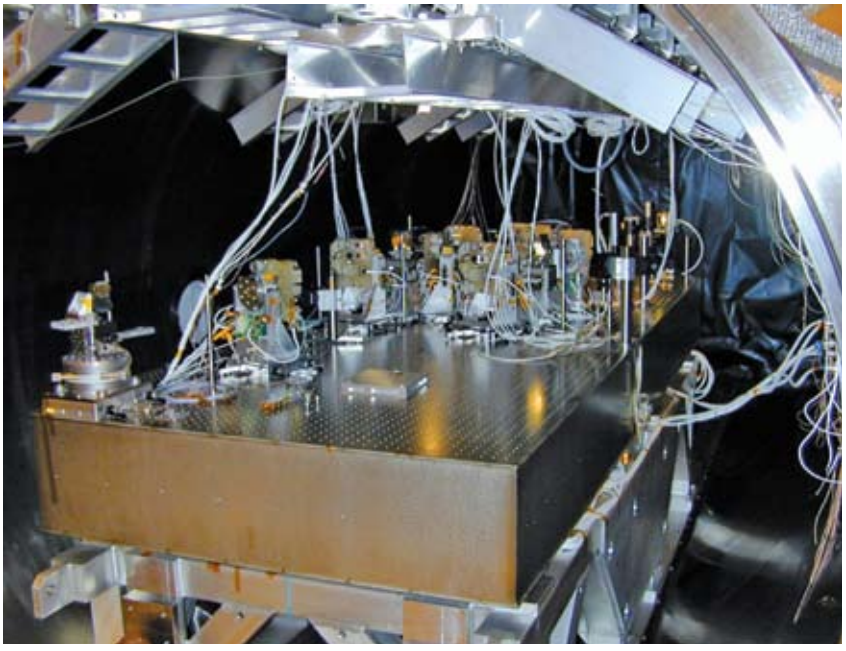

Figure 19-9. The Kite testbed shown here in the vacuum chamber, demonstrated that a collection of fiducials separated by many meters can be monitored with pm accuracy. (From Laskin 2006.)

Figure 19-10. Kite's metrology gauges, shown here during a one-hour quasi-static run, are seen to be highly accurate, as evidenced by the black trace. The full extent of their unprecedented accuracy can be seen in Figure 19-11.

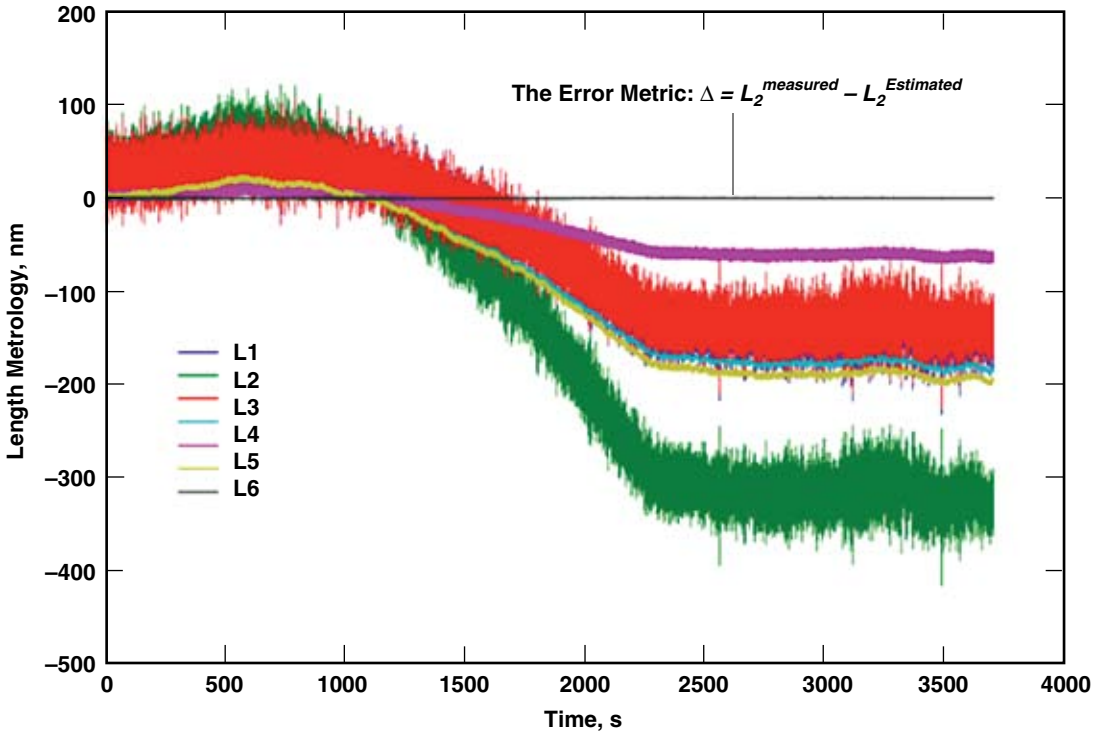

Figure 19-11. SIM Lite's chopping scheme is seen in this quasi-static test to be highly effective in bringing errors down to the required pm class.

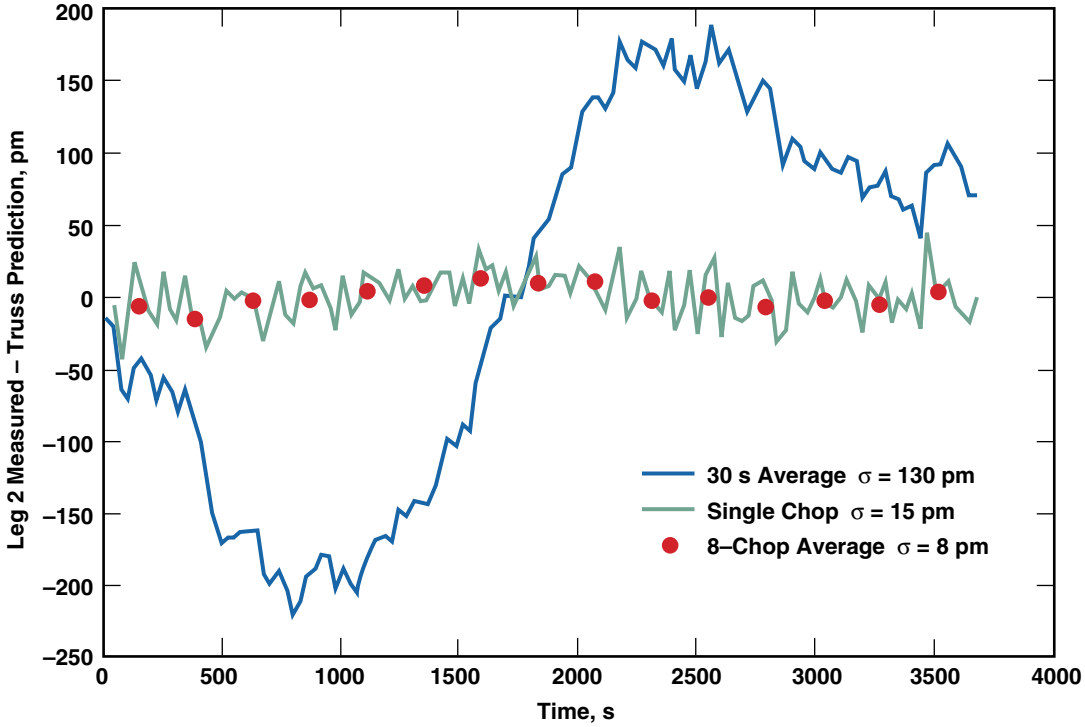

away and back. The Kite narrow-angle visits consist of two cycles of four chops each, with one reference star per chop. The RMS error for the eight-chop visit is measured to be 5.6 pm. This demonstrates that, even in the highly demanding circumstances of the narrow-angle observing scenario, the external metrology truss can meet its requirements.

19.4 The Guide-2 Telescope Testbed

One of the innovations that has enabled the lower-cost SIM Lite architecture is to use a precision star tracker to perform the Guide-2 function. To meet the requirements for μas astrometry, the Guide-2 telescope (G2T) must achieve an unprecedented 50 μas star-tracking capability. The greatest challenges to achieving this level of performance are expected to be (1) thermally induced deformations of the telescope system, and (2) measurement error in the angle metrology system. To develop this technology and demonstrate that such an instrument is feasible, the G2T testbed was built in the same vacuum chamber that had earlier contained the Kite testbed (Figure 19-12).

On SIM Lite, G2T consists of a 30 cm siderostat (Figure 19-13) and a 30 cm confocal beam compressor, similar to the other telescopes in both the science and Guide-1 interferometer. Starlight collected by G2T propagates directly to a CCD-based pointing sensor. As the attitude of SIM Lite changes in inertial space, the G2T siderostat mechanism tracks the guide star, maintaining the star spot at the optimal position on the CCD. An angle metrology gauge (aMet) tracks the siderostat motions required to keep lock. The star tracker output is the sum of the pointing sensor signal and the angle metrology.

The testbed layout is shown in Figure 19-14. White light is injected and collimated using an off-axis parabola and propagates through the beam compressor (7:1) to the siderostat in a retroreflecting position. The beam is returned to the fine-steering mirror (FSM) and focused on the pointing sensor. The optomechanical drift of the entire optical train is compensated by the FSM and measured by the aMet. By placing the siderostat in the retro configuration, G2T directly measures its own angular stability.

The angle metrology gauge is perhaps the most innovative feature of G2T. Figure 19-15 shows the aMet architecture. Based on the heterodyne metrology approach developed for internal and external metrology, aMet monitors the angle of a reflecting surface by probing the distance to three or four reference points (corner cubes) mounted on the surface (Figure 19-16).

In the initial phase of this testbed, the siderostat is not actuated. With the siderostat in retro position, the FSM is used to lock the artificial star (fiber tip) image on a fixed spot on the CCD pointing sensor. The aMet gauge tracks the tip/tilt of the FSM independently. In SIM Lite, the pointing detector and aMet readings together are used to provide the measurement of the G2T rigid-body rotations. In this testbed configuration, however, they measure the instrument's internal errors.

Figure 19-17 shows results from a typical G2T run, three hours in this case, under quasi-static conditions. The orange trace is the pointing sensor reading in real time under closed loop control. The blue trace is the aMet reading of the FSM position as it is controlled to lock the star image on the pointing detector. Together these two readings capture all the drift and noise in the system. In a recent 200-hour run processed according to SIM Lite's narrow-angle observing scenario, the measured G2T error was found to be less than 30 μas. This surpasses the required G2T performance for SIM Lite.

Figure 19-12. The G2T testbed, shown here in the vacuum chamber, has demonstrated star-tracking capability at an unprecedented 30 μas level. (Hahn et al. 2008)

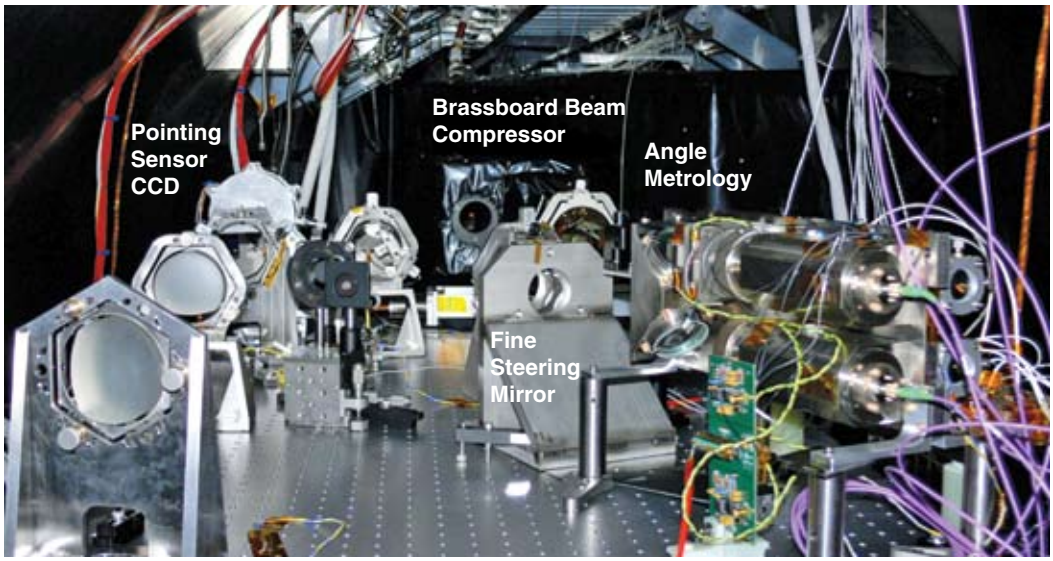

Figure 19-13. The brassboard siderostat in G2T uses a sophisticated corner cube design that allows μas level angle metrology. (Laskin 2006)

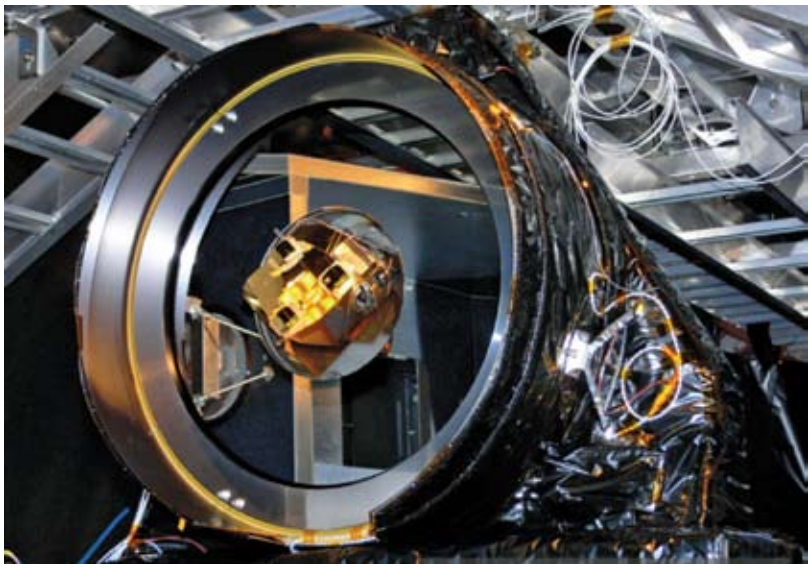

Figure 19-14. The G2T testbed has all the essential optical elements of the Guide-2 telescope, including a brassboard beam compressor and a brassboard siderostat. (Hahn et al. 2008)

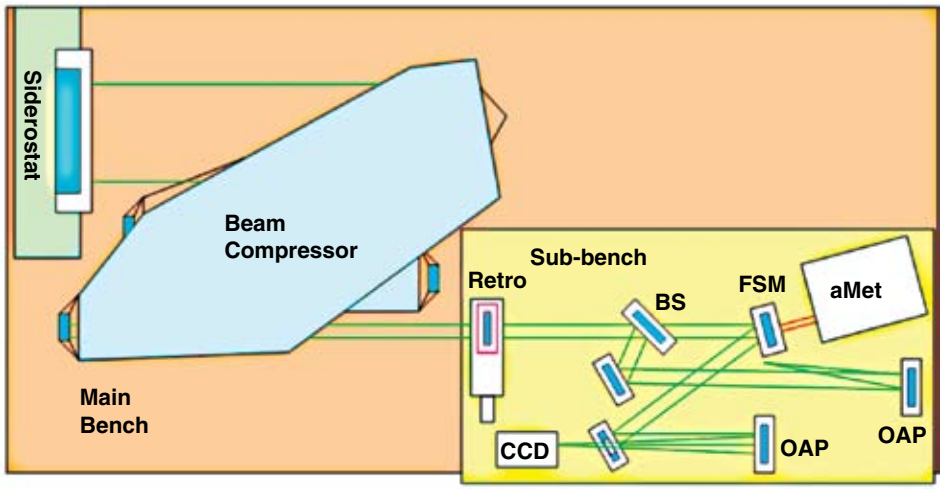

Figure 19 15. The angle metrology (aMet) system uses the proven heterodyne architecture of all SIM Lite metrology systems. (From Hahn et al. 2008.)

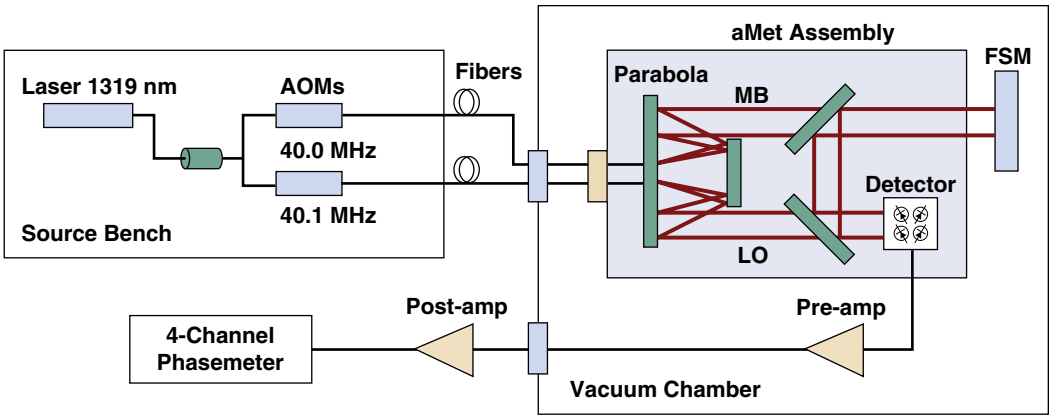

Figure 19-16. The aMet beam launcher is based on the internal metrology brassboard with a modified photo detector assembly (inset).

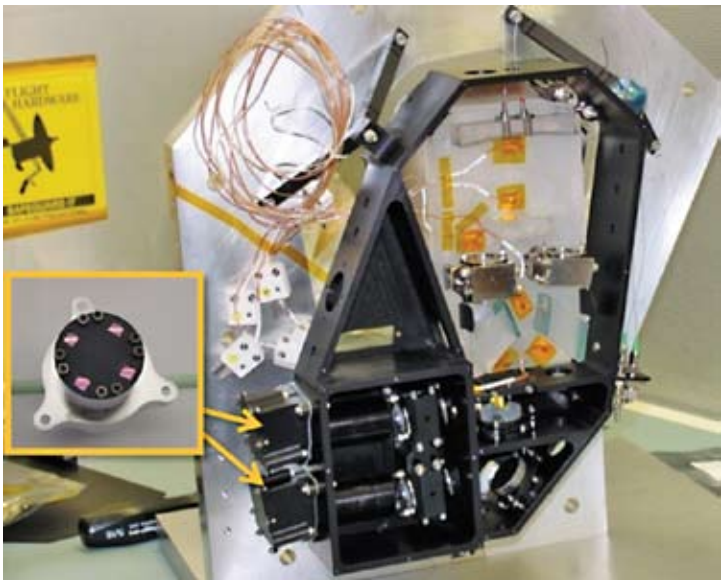

Figure 19-17. Pointing sensor and aMet angle measurements from a typical G2T run show that the FSM is effectively keeping the (orange) centroid locked on the CCD while the siderostat, under flight-like thermal conditions, undergoes mas level drift (blue).

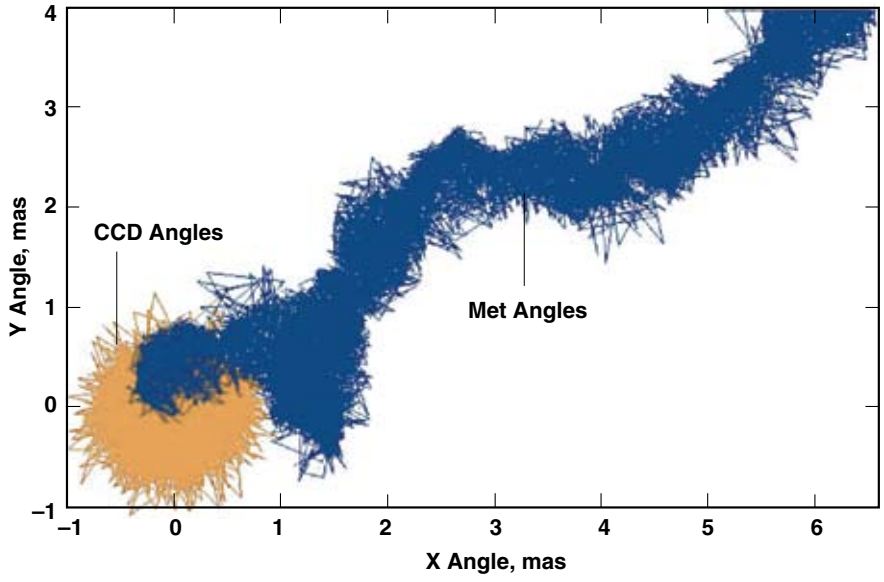

19.5 The Three-Baseline System-Level Testbed

As seen in Chapter 18, precision fringe measurement requires high fringe contrast or visibility. The dynamic contributions to a reduction of visibility are jitter in the relative path length and pointing of the combined beams. In particular, when the astrometric target is dim, active stabilization of the pathlength and pointing using conventional closed-loop techniques is not adequate due to photon noise. In these cases, other sensors are needed to predict the required pathlength and pointing corrections (so-called pathlength feed-forward and angle feed-forward) to be applied while the observation and integration of photons is in progress.

The STB-3 testbed was designed to capture the dynamics and control aspects of SIM. While the testbed was designed and operated prior to the innovations that led to SIM Lite, virtually all of the demonstrations and lessons learned are valid to the new design. STB-3 made it possible to develop the approach to pathlength and pointing control, as well as feed-forward, in the presence of disturbances higher than expected for SIM Lite. It also facilitated validation of a nm-level dynamics and control model for the instrument. Figure 19-18 shows the testbed with the collector bays on the near and far ends, and with the combiner bays in the center of the picture. The testbed is operated in air, since for control purposes nm-class performance is adequate.

Figure 19-19 shows the major system components of STB-3. The Precision Support Structure (PSS) is a 9-m-long, flight-like, flexible structure (longer than SIM Lite). It is capable of supporting an attitude control system (ACS) module, one of the main sources of jitter in the system. The two collector bays (east and west) are where the telescopes are housed, together with relay optics, fine-steering mirrors for pointing, and external metrology beam launchers. The beam launchers measure how the interferometer fiducials move relative to each other as a result of thermal drift and dynamic disturbances. The beam combiner pallets contain the combining optics, internal metrology, the delay lines, and the tracking cameras that monitor pointing.

Figure 19-19 also shows the pseudo star system. It is an inverse Michelson Interferometer that is used to generate collimated, in-phase wavefronts to both collector bays. A diffraction grating splits the pseudo star beam at each end into simulated wavefronts from three stars in the sky 15.4 degrees from each other: the science, Guide-1 and Guide-2 stars. The test article is mounted atop three, 1/2-Hz-class isolators designed to render the system quasi free-free in six degrees of freedom.

During SIM Lite science operations, fringe motion occurs when the attitude of the instrument varies within the deadband of the ACS and when the structure deforms as a result of varying thermal loads in normal operation. In SIM Lite, the fringe must be stabilized to less than 10 nm RMS or lower in order to reach μas-class accuracy in each visit. Modeling of the ACS system performance shows that a disturbance rejection of at least 40 dB (i.e., a factor of 100 in amplitude) is required in the frequency range 0.1 to 1 Hz.

To attain this level of suppression, SIM Lite will use a combination of passive and active methods. The passive method is dual-stage isolation of the reaction wheels in the spacecraft, which are the largest source of jitter (>10 Hz). The active method is a technique called pathlength feed-forward (PFF), mainly used to reject rigid body motion (<10 Hz) and thermal drift. The science interferometer itself cannot be used to compensate for these disturbances, as its targets are often too dim and generate photon rates that are too low for sufficient sensory bandwidth.

In the PFF technique, the guide instruments are used to pinpoint the attitude of the instrument with respect to the target star of interest. To account for jitter and thermal distortions among the instruments, the external metrology system is used to tie the guide data to the science interferometer.

Figure 19-18. The STB-3 testbed emulates the full SIM Lite instrument and features a flight-like flexible structure.

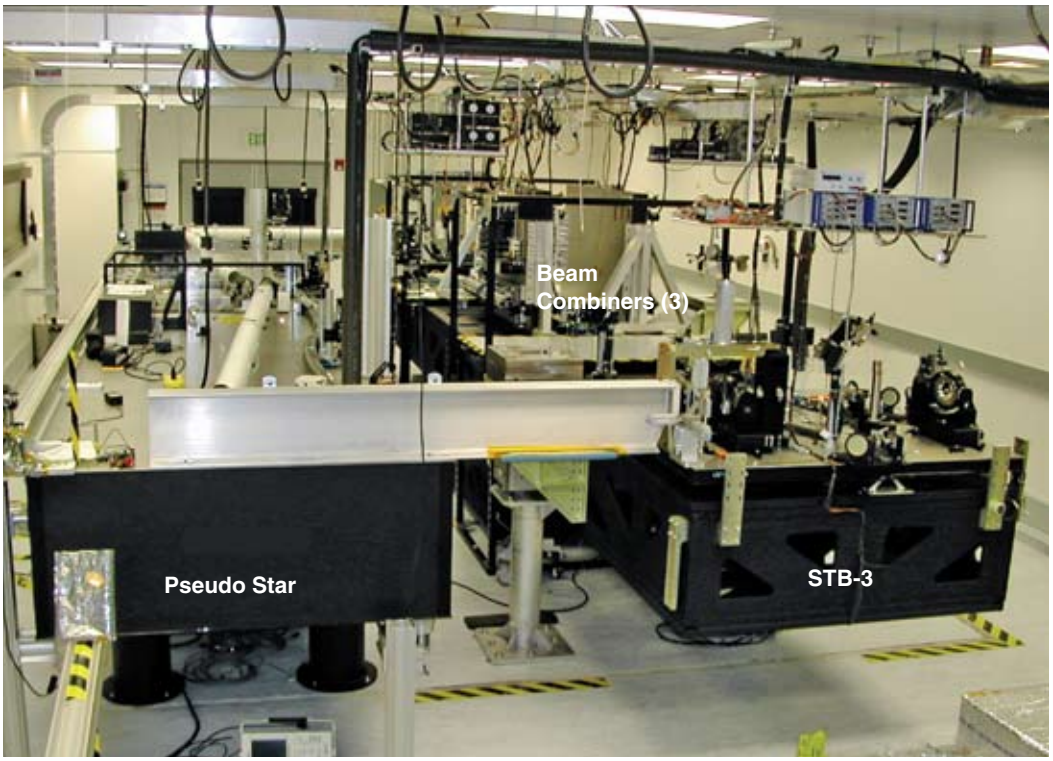

Figure 19-19. The STB-3 test set-up, shown here, allows for the illumination by three simulated stars so that full system-level tests can be conducted. (From Laskin 2006.)

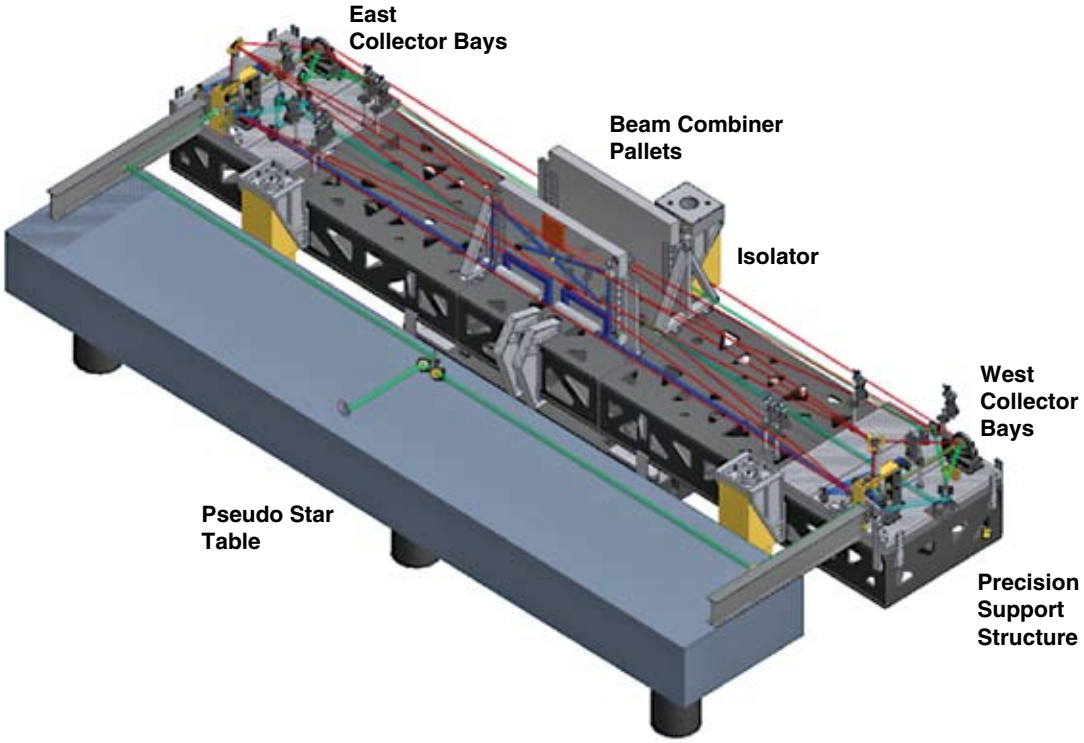

Figure 19-20 shows a 20-minute fringe-tracking experiment during which the ACS error simulator (a voice-coil acting against the structure) injected a harmonic ACS disturbance resulting in about 2200 nm RMS of science delay at 0.01 Hz (blue trace). The figure also shows the phase residual for the science interferometer under PFF control (green trace). To simulate the on-orbit situation, data from the science fringe detector are not used in tracking the fringe. The phase jitter over all frequencies is seen to be 38 nm RMS, including both drift and broadband contributions. The drift in the PFF residual contributes about 26 nm RMS to the total error, and it is largely due to drift in the internal metrology sources (all three interferometers in STB-3). The flight metrology design has been shown to have much less drift than this. The atmosphere's contribution to the low-frequency error (i.e., <1 Hz) is estimated to be in the neighborhood of 6 to 10 nm RMS (this estimate is actually based on external metrology data).

Figure 19-21 shows the power spectral density for the data. The disturbance applied at 0.5 Hz is seen to be rejected by 50 dB, better than the requirement. At 0.01 Hz, the rejection is about 60 dB. Here the experiment was limited by the laboratory ambient noise floor on the one hand and the maximum available ACS range on the other. The experiment clearly shows that the PFF performance exceeds all requirements (i.e., better than 40 dB of rejection at a frequency in the 0.1 to 1.0 Hz band). STB-3 has verified that the dynamics and control challenges of space-based stellar interferometry have been met and SIM Lite is ready for flight design.

19.6 The Thermo-Opto-Mechanical Testbed

The Thermo-Opto-Mechanical (TOM) testbed (Figure 19-22) was designed to demonstrate that SIM Lite's collectors can meet their stringent wavefront stability requirements under flight-like thermal conditions. Each collector includes a siderostat and a beam compressor. In the center of the siderostat is a double corner cube (DCC) that serves as a fiducial for the metrology system that determines the pathlength differences in the interferometer. The beam compressor (Figure 19-23) is an off-axis confocal telescope. Using brassboard versions of these components, the testbed has shown that SIM Lite will meet its unprecedented thermal requirements.

In SIM Lite's science and Guide-1 interferometers, the internal metrology footprint occupies the central region of each optic while the starlight occupies the surrounding annulus. This arrangement, which is optimal in many respects, does make the instrument sensitive to changes in wavefront error (primarily power/defocus) over the course of a measurement. In the case of the all-important siderostat, the central part contains a DCC. Any "piston" motion of the DCC relative to the siderostat mirror can cause an error. The optical path difference between starlight and metrology through the siderostat and the large compressor optics must be stable to tens or hundreds of pm, depending on the type of SIM Lite observation.

The primary source of wavefront instability in SIM Lite is thermal disturbance, and the main on-orbit thermal disturbance is expected to be from the change in the relative position of the Sun with respect to SIM Lite. The typical observational scenario will generate about 7 degrees of episodic spacecraft motion every hour in order to slowly scan the entire sky. The next most important thermal disturbance occurs with the change in the orientation of the siderostat relative to the rest of the collecting hardware when it is articulated. The siderostat will acquire light from stars anywhere in its 15 degree FOR. These two thermal disturbances are simulated in TOM using its liquid nitrogen thermal shroud. The temperature variations are produced by simulating the operational scenarios for the flight system and then generating thermal profiles for the shroud heaters that would produce a similar environment for the siderostat. The objective of the testbed is to show that the Science collector and Guide-1 collector, in the presence of flight-like thermal conditions, will not cause wavefront thermal instabilities that exceed the error budget allocations. Another important goal of the testbed is to develop an integrated thermo-opto-mechanical model and validate its predictions.

Figure 19-20. The STB-3 testbed demonstrates that pathlength feed-forward can suppress large fringe-delay errors (blue) down to the nm level (green). (From Laskin 2006.)

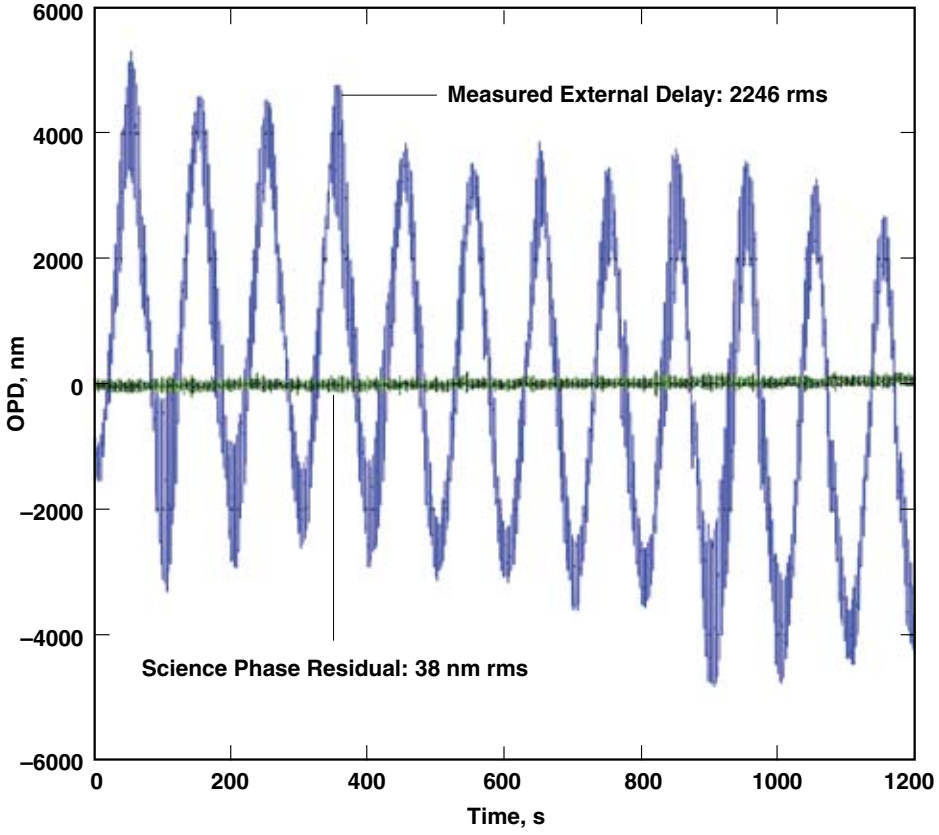

Figure 19-21. A power spectral density of STB-3 results shows the excellent rejection of disturbance in the region of greatest interest (>60 dB at 0.01 Hz to >50 dB at 1 Hz), surpassing SIM Lite's stabilization requirements. (From Laskin 2006.)

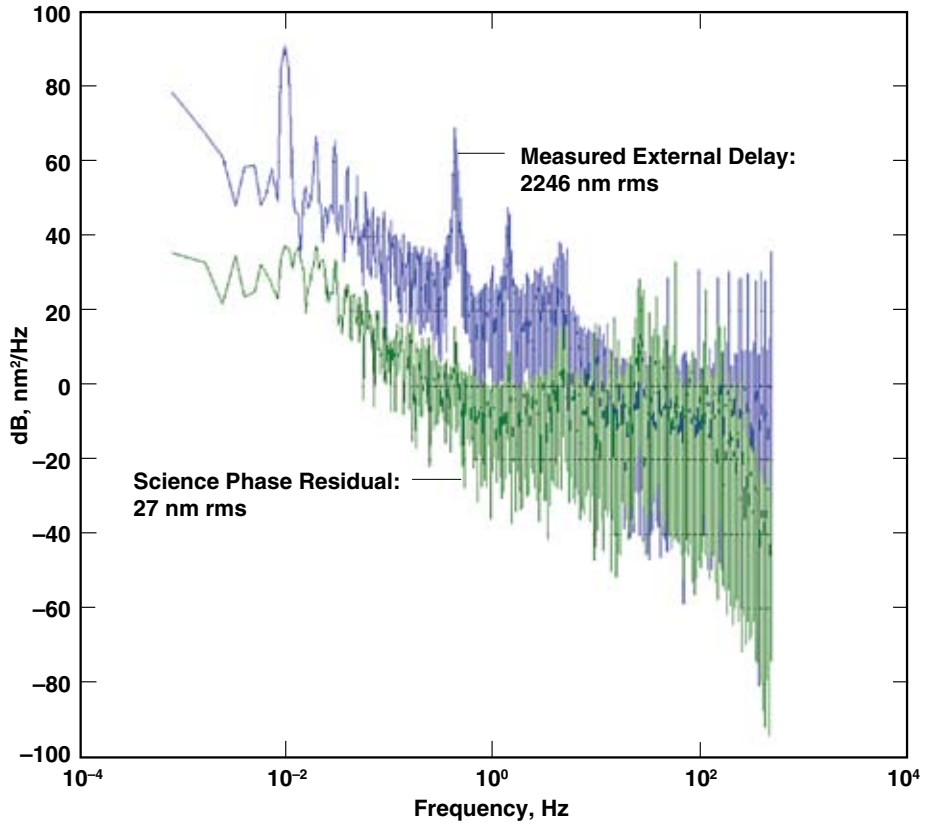

The test article includes a brassboard siderostat and brassboard beam compressor monitored by a highly precise multisensor metrology gauge called the Common Optical Path Heterodyne Interferometer (COPHI). COPHI was the original prototype metrology gauge that led the way to all the SIM Lite pm-class beam launchers. For this testbed, the COPHI detector was modified to monitor OPD errors over a number of points across the siderostat, including the DCC at its center. A schematic of the testbed and a view of some of the optics is shown in Figure 19-24.

TOM tests involved multihour runs where the testbed thermal environment was made similar to expected SIM Lite flight levels. The test metric is the average difference between the central metrology reading and nine annular readings (Figure 19-24).

For the Guide-1 collector test, the chopping fold mirror is in the retro position with respect to the COPHI sensor such that the beam compressor becomes the main test article. Figure 19-25 shows the result of a typical data run. One can see a strong correlation between the thermal variation and the optical response in the data shown in the figure. The slow downward drift and the diurnal cycle of the temperature suggest a 3 nm/K linear thermo-opto-mechanical sensitivity of the compressor (single path) that is consistent with the thermal model predictions.

The OPD was processed from the raw data according to the narrow-angle observing scenario (the more limiting scenario) and the narrow-angle error was found to be 5.4 pm. Separate testing showed that the number was in fact dominated by the error in the test set-up, rather than the test article itself. For example, COPHI's noise contribution was found to be 3 pm, leaving 4.5 pm as the measured thermal stability error of the Guide-1 collector. Thus the Guide-1 collector exceeds the SIM Lite wavefront thermal stability requirements.

For the science collector test, the COPHI sensor measured the OPD stability, including the siderostat together with the beam compressor. The results of tests suggested that the narrow-angle performance of the science collector at the inboard bay (nearest the rocket booster) of the SIM Lite structure is 9.5 pm, and 8.7 pm for the case of outboard bay. These testbed performances are near the required levels for the SIM Lite mission. Further testing indicated that the stability of the COPHI measurement system (which is ground-support hardware) limited the ultimate performance test of brassboard hardware. In these tests, the system was thermally overdriven and the results confirmed that the test article's true thermal sensitivity is significantly better than SIM Lite requirements.

Beyond the direct performance tests, TOM was also used to validate SIM Lite's integrated thermo-opto-mechanical model. The overdrive tests were used to correlate the model with the raw data. Figure 19-26 shows the typical results from a 16-hour data run. The TOM-measured OPD is shown in dark blue (the spikes in the data are glitches in COPHI and not physical). The OPD measurements showed a strong temperature dependence, as expected. The other traces are integrated model calculations with various conditions. Three varieties of modeling are shown in the figure: fully modeled (orange), in which thermal model predictions were put into the structural model to generate OPD outputs; partially modeled (red), in which an empirically measured sensitivity of the OPD to the siderostat temperature (dOPD/dT) was used; and empirically modeled (green), in which the measured dOPD/dT number (6 nm/K) was simply multiplied by the measured temperature changes.

The thermal models using the best available inputs predicted the relevant parameters (peak-to-valley temperature change and rate of change) to within 60 percent prior to any attempts to adjust uncertain model parameters to fit the experimental data. For most components of interest, except for the DCC, the model over-predicted the temperature swings and rate of change. The over-prediction is preferable to under-prediction because it provides margin against design or modeling errors.

Figure 19-22. The TOM testbed includes a brassboard siderostat and double corner cube (gold colored) centered in the siderostat mirror. (From Laskin 2006.)

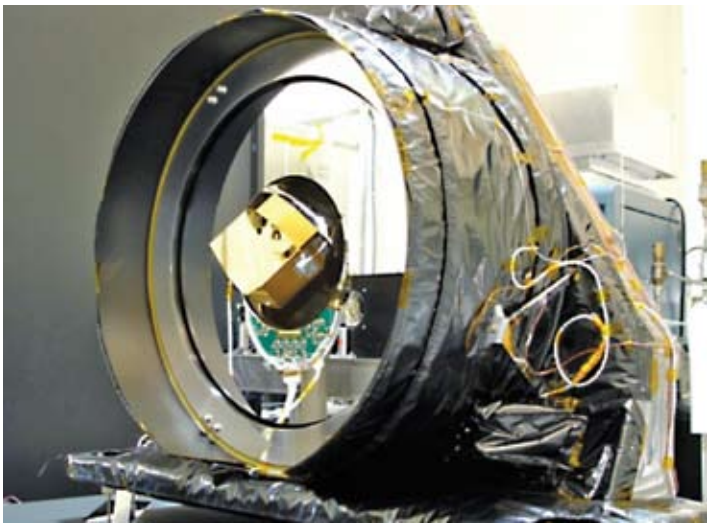

Figure 19-23. The brassboard beam compressor used in TOM has shown excellent wavefront stability.

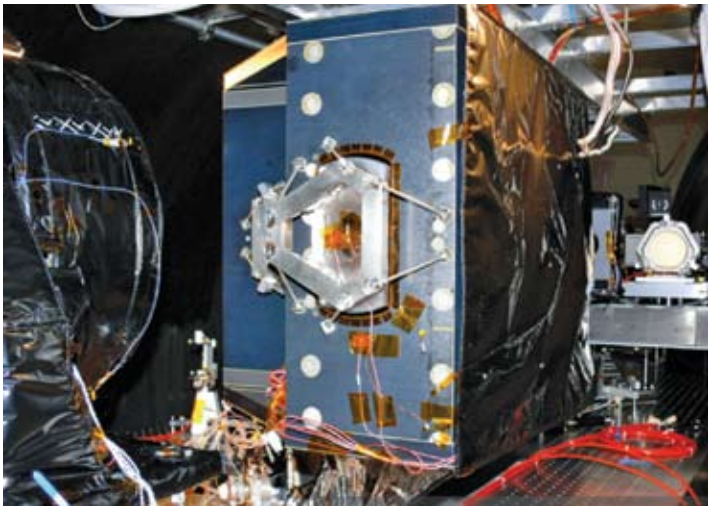

Figure 19-24. The TOM testbed layout (left) and view from the fold mirror (right).

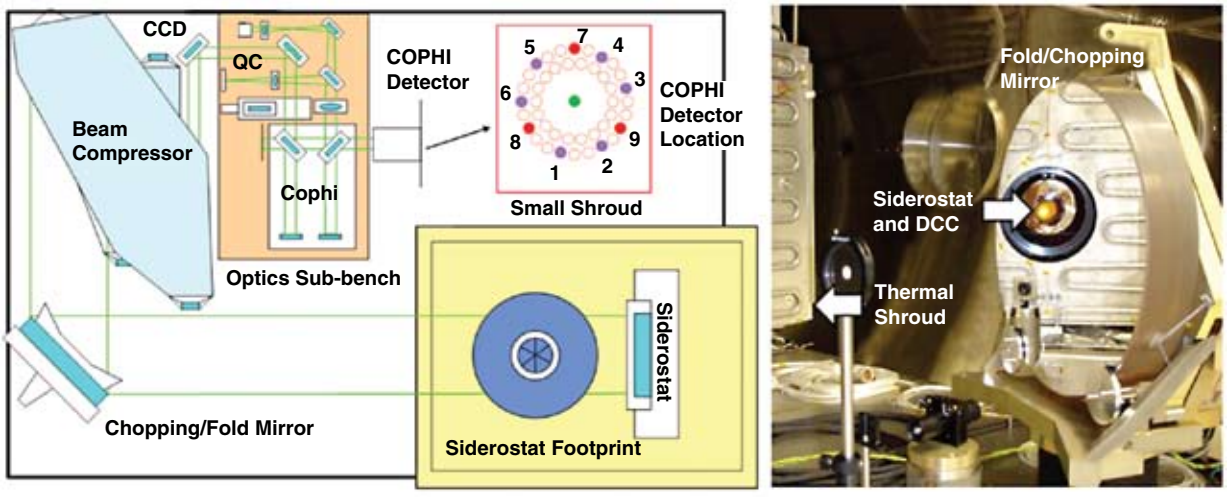

Figure 19-25. The OPD versus temperature (magenta circles) measurement correlates well with the temperature profile (all other traces) and is indicative of the Guide-1 collector performance. M1, M2, and M3 re the three main mirrors in the beam compressor; COB stands for collector-outboard side.

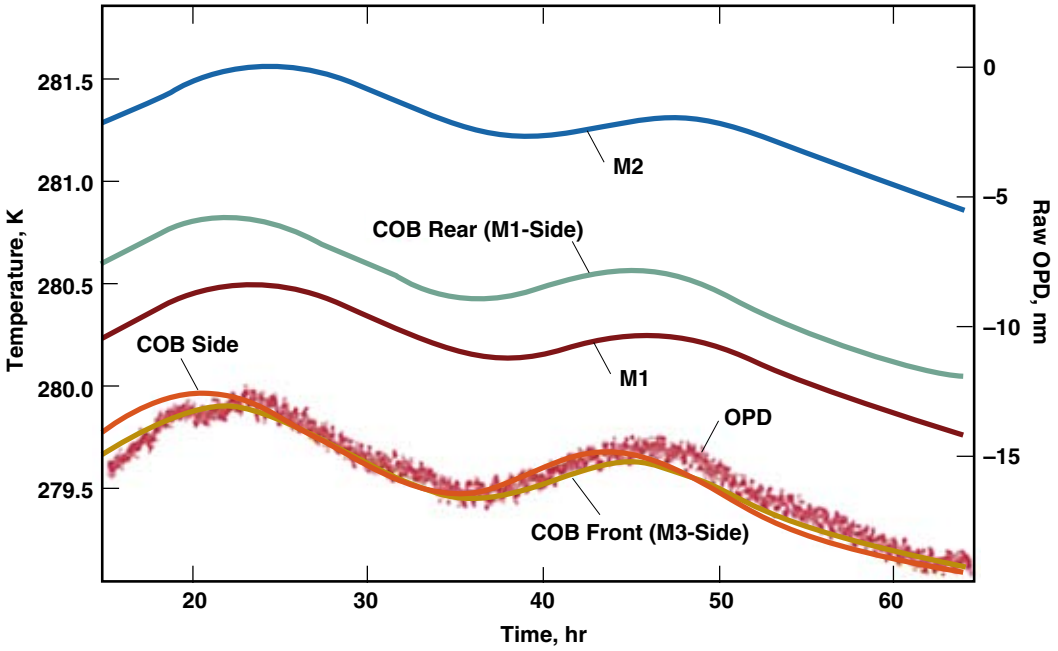

Figure 19-26. The SIM Lite integrated thermo-opto-mechanical models perform well in predicting the dependence of OPD on temperature. (From Laskin 2006.)

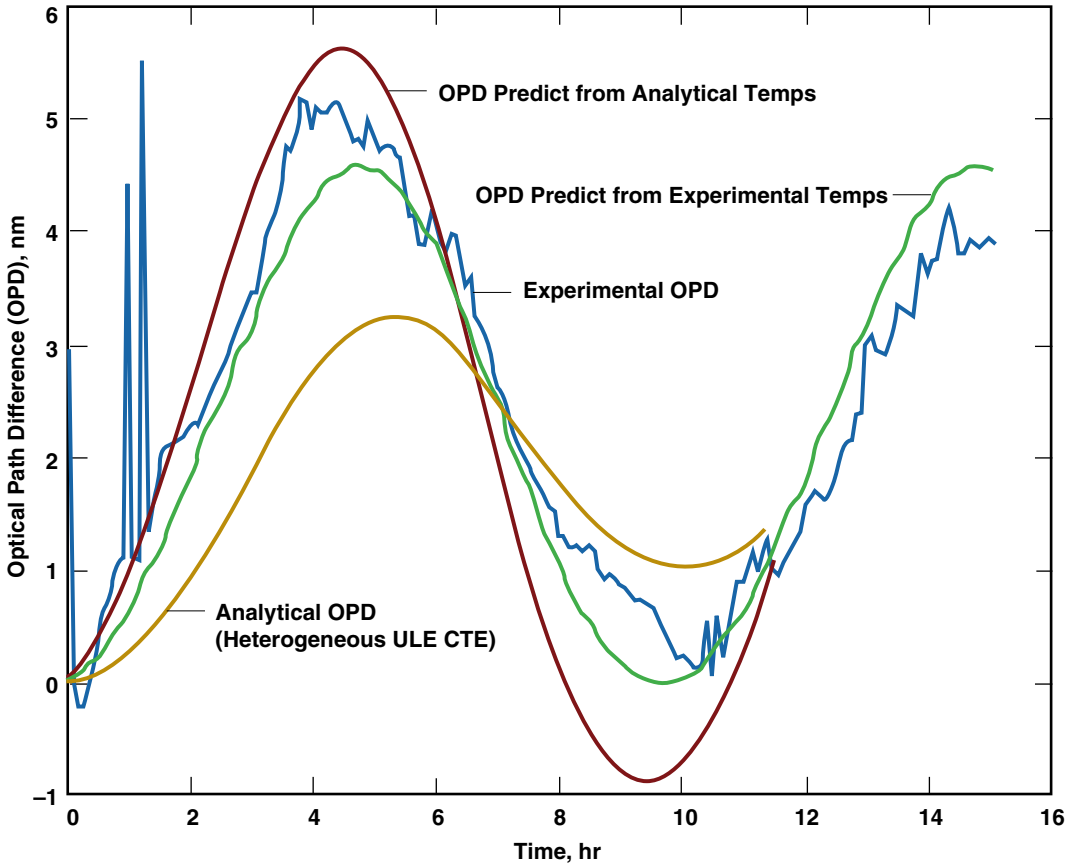

The structural models, though fairly sensitive to accurate knowledge of material parameters, particularly the coefficient of thermal expansion (CTE), provide valuable performance predictions for flight development. Prior to model correlation, the structural model of the siderostat under-predicted by a factor of about three. After modifying the CTE of the ultra-low-expansion (ULE) glass in the model to be more consistent with the properties of the real glass, including inhomogeneity, the model under-predicted by a smaller factor of about 1.6. Understanding the modeling uncertainty factor is important for developing design margins for the flight system.

Overall, the TOM testbed consistently demonstrated performance close to or better than the goal levels of the Science and Guide-1 collectors. In all cases, the test results appear to be limited by the noise floor of the ground support measurement system rather than the actual performance of the flight-like test articles.

19.7 Completeness

The ultimate test of completeness is a full-up test article that matches the operation of the flight article in all its details in an environment that is completely flight-like. With SIM Lite, as with all the next generation large instruments, this is an ideal increasingly impossible to realize. SIM Lite has benefited from an impressive array of testbeds, only a few of which have been highlighted in this book. These testbeds have come very close to reaching the ideal at the level of the instrument's fundamental sensors. That is, MAM replicates all the complex operations involving a single, pm-class stellar interferometer; Kite does the same thing for the external metrology system, and G2T captures the most important, previously untested aspects of the Guide-2 telescope sensor. TOM shows that the all-important thermal errors are well handled by the SIM Lite design. STB-3 shows that the control authority exists to stabilize the fringe to the levels required for pm fringe measurement. Together these testbeds have made a strong case, confirmed by a very thorough and independent technical review process, that the technology for each of the sensors is at hand. The same review process also examined the entire SIM Lite approach, asking whether any "holes" might exist in considering the performance of the full instrument. What follows is a result of this examination, which took place over the last few years.

At the heart of SIM Lite's architecture is a provision to minimize the number and impact of "holes" by requiring that the instrument sensors obey the principal of separability. This means that if the each of the four fundamental sensors work to the levels required by the error budget, the whole instrument shall meet its mission goals. There are a number of situations where separability can in principle be violated. These ultimately all involve pure sensing errors. SIM Lite addresses these cases through measurement, calibration, and placement of tight requirements on mechanisms that feed any of these violations. The three categories of situations where separability can be violated are:

I. Second-order errors involving a motion and a knowledge error.
II. Instrument fiducials being sensed inconsistently by different sensors.
III. Cross-talk or corruption of one sensor due to another sensor.

Second-order errors were discussed in the error budget, Chapter 18. These are arguably the most important violators of separability. The approach to minimize these errors involves tight requirements on the motions involved, and calibration of the parameters whose errors can contribute to a given second-order error. For the example described in Chapter 18, the error due to the coupling of ACS motion and baseline nonparallelism is brought within allocations by placing tight ACS deadband requirements (<0.2 arcseconds over 10 minutes) and at the same time placing tight absolute metrology requirements (<3 μm absolute error per metrology link).

The second category of separability violators involves the instrument's fiducials. The double corner cubes, in particular, are the most fundamental reference points on the instrument since they define the ends of the science baseline. However, the very fact that they are double cubes means that the science interferometer sensor's internal metrology probe sees one cube, while the external metrology system sees another. Since it is not practical to make the distance between the vertices of the two corner cubes zero, a motion of the DCC during retargets from one star to another couples to this non-common-vertex error (NCVE) to create a type of second-order error. (This error happens to be book-kept in the error budget under external metrology's allocation. Otherwise it would naturally belong under second-order errors.) A specific testbed called NCVE showed that submicron absolute measurement of the NCVE is feasible. Later, analysis and modeling showed that on-sky calibrations can also provide this important parameter, so that this source of separability can meet its allocation using the simpler approach.

The final category of separability violators involves crosstalk between the sensors. This is only a significant issue between internal metrology (part of the Science and Guide-1 interferometer sensors) and external metrology. Here the heterodyne laser beam from internal metrology could potentially leak into the external metrology beam launcher's detector, and vice versa. To ensure this error is small, a specific test was done that mimicked the geometry of a typical external metrology link with respect to an internal metrology beam incident on the same corner cube. The measured cross-talk was found to be significantly smaller than the allocation. Had this cross-talk been a significant issue, a relatively simple mitigation approach would have been to use different heterodyne frequencies for internal and external metrology, taking advantage of filtering in the electronics to eliminate this error.

At the heart of SIM Lite's architecture is a provision to minimize the number and impact of "holes" by requiring that the instrument sensors obey the principal of separability. This means that if the each of the four fundamental sensors work to the levels required by the error budget, the whole instrument shall meet its mission goals.

To summarize the answer to separability, SIM Lite, through an extensive and independently reviewed technical program has shown that the individual sensors meet their requirements (the pm technology testbeds) and further that the areas where errors could occur in the interplay of the sensors are each mitigated through tests, measurements, and calibrations.

A final note is appropriate on the important question of the SIM Lite data flow and its processing to create a complete astrometric result. SIM Lite has developed an extensive array of modeling tools that have been validated using the testbeds. These primarily include the instrument model and the SIM Lite mission simulator (SIMsim).

The instrument model captures outputs from all sensors and motions in the fundamental fiducials of the instrument. It uses testbed data to create empirical pseudo data with correct noise characteristics, and flows the data into telemetry. It simulates its subsequent processing up to the point of arriving at regularized delays. Using the delays, the instrument model applies realistic observing scenarios to show that the predicted instrument performance is consistent with testbed results in affirming that error budget allocations can be met.

SIMsim is a computer model that starts at the level of individual telemetries and simulates the entire mission, including actual star characteristics and locations from star catalogs, Sun and Earth exclusion, slew times, and calibration-related observations. It simulates the complete calibration and post-processing to the level of final astrometric products such as position, proper motion, and parallax. SIMsim was instrumental in identifying zonal astrometric errors and verifying that the use of quasars was effective in minimizing them. It also is an indispensable tool in determining the schedule of observations and the optimization of the schedule for maximum observing time and minimum calibration errors.

Overall, SIM Lite's development has placed a high emphasis on retiring risks and ensuring completeness. The full array of tests and modeling that has led to successful completion of all of the NASA-required technical milestones is described in the SIM technology plan volumes submitted to NASA.

References

Hahn, I., Sandhu, J., Weilert, M., Smythe, R., Nicaise, F., Kang, B., Dekens, F., and Goullioud, R., 2008, Proc. SPIE Vol. 7013, 70134W.

Hines, B. E., Bell, C. E., Goullioud, R., Spero, R., Neat, G. W., Shen, T. J., Bloemhof. E. E., Shao, M., Catanzarite, J., and Regehr, M., 2003, Proc. SPIE, Vol. 4852, 45.

Laskin, R.A., 2006, IAC-06-A3.P.1.05.